Responses of spatiotemporal chaos to oscillating forces

Misato Iino,[1] Yoshiki Hidaka,[1,*] Fahrudin Nugroho,[2] Rinto Anugraha,[2] Hirotaka Okabe,[1] and Kazuhiro Hara[1]

[1]*Department of Applied Quantum Physics and Nuclear Engineering, Faculty of Engineering, Kyushu University, Fukuoka 819-0395, Japan*

[2]*Physics Department, Faculty of Mathematics and Natural Sciences, Gadjah Mada University, Yogyakarta 55281, Indonesia*

(Received 23 March 2015; revised manuscript received 23 May 2015; published 22 July 2015)

The responses of soft-mode turbulence, a kind of spatiotemporal chaos seen in electroconvection of a nematic liquid crystal, to alternating-current magnetic fields is investigated to uncover the dynamical properties of spatiotemporal chaos. The dynamical responses can be measured by an order parameter, $M_p(t)$, which indicates ordering in the convective roll pattern induced by the magnetic field. Determined by properties of the liquid crystal in a magnetic field, $M_p(t)$ oscillates in accordance with the square of the magnetic field. The relaxation time of the system was obtained by fitting the frequency dependence of the complex susceptibility for the pattern obtained from the oscillation of $M_p(t)$ to the Debye-type relaxation spectra. However, for the high-frequency regime, the susceptibility deviates from the spectra because slow and large fluctuations of $M_p(t)$ contribute to the oscillation. The properties of this type of fluctuation were investigated by introducing a dynamic ordering parameter defined as the period average of $M_p(t)$.

DOI: 10.1103/PhysRevE.92.012916 PACS number(s): 05.45.−a, 47.52.+j, 47.27.−i, 61.30.−v

I. INTRODUCTION

In general, to investigate the physical properties of a system, the responses to external forces are chosen for measurement. The response is directly proportional to the external force if it is sufficiently small. In this case, the physical properties can be described as the response functions within the linear response theory [1]. If the physical properties depend on time, responses to periodically oscillating forces are useful means to investigate them. Such responses can reveal the dissipation and the absorption of energy of the system.

One interesting phenomenon is spatiotemporal chaos (STC), which is observed in nonlinear nonequilibrium systems with spatial degrees of freedom. Here STC is defined as weak turbulence which is locally ordered but globally disordered [2–4]. The topic of the present study is soft-mode turbulence (SMT), which is one aspect of STC encountered in electroconvection of a nematic liquid crystal (NLC) with homeotropic molecular alignment. In the homeotropic nematic system, because the director $\mathbf{n}$ is perpendicular to the electrodes (x-y plane), continuously rotational symmetry in the x-y plane is maintained. Applying a voltage higher than a certain V_F to the system along the z axis, an instability, called the Fréedericksz transition, occurs whereby the director $\mathbf{n}$ tilts from the z axis. With the appearance of the instability, the continuously rotational symmetry is thereby spontaneously broken. Here, we define a two-dimensional (2D) director $\mathbf{C}(\mathbf{r})$, where $\mathbf{r} = (x,y)$, as the projection of $\mathbf{n}$ onto the x-y plane. The azimuth $\phi(\mathbf{r})$ of $\mathbf{C}(\mathbf{r})$ behaves as a Nambu-Goldstone (NG) mode [5]. Therefore, the excitation energy for the fluctuation corresponding to zero wave number for $\phi(\mathbf{r})$ is 0. Moreover, applying a voltage above a threshold V_c, electroconvection is generated by the electrohydrodynamic effect [6] and a convective roll pattern appears. Then, as $\phi(\mathbf{r})$ behaves as an NG mode, $\mathbf{C}(\mathbf{r})$ rotates because of the viscous torque from the convective flow [7]. This rotating $\mathbf{C}(\mathbf{r})$ changes the directions of each of the convection rolls by the electrohydrodynamic effect. Consequently, the directions of convection are always unstable by such an interaction. This unstable state is the SMT in which local convective rolls are maintained and the direction of the convective rolls spatiotemporally varies globally [see Fig. 1(a)] [8]. Here, we define the local wave vector $\mathbf{q}(\mathbf{r})$, which is perpendicular to the local convective rolls, and its azimuth $\psi(\mathbf{r})$.

The SMT induced by the nonlinear interaction between the convective flow and the director occurs in the weakly nonlinear regime because the director behaves as the NG mode. Therefore, singularity, anisotropy, and intermittency are lower than those of other kinds of STC. For this reason, the SMT is regarded as an ideal feature in STC to research fundamental properties of STC. STC can be regarded as fluctuations induced by nonlinear interactions; their properties have been studied from the viewpoint of statistical mechanics. With respect to SMT, the temporal correlation and memory functions describing the dynamics of the convective patterns [9,10] and nonthermal Brownian motion driven by the fluctuations have been studied [11–14].

In the present study, we investigate the response of the SMT to external fields. Let us consider a substance which is composed of polar molecules with permanent dipoles as a familiar example. Because there is competition between disorder with the increase in entropy for the molecular alignment and order from the coercive torque for the dipole moment by an electric field, a finite value for an order parameter is determined corresponding to temperature and strength of the electric field. In contrast, applying a magnetic field to the homeotropic nematic system after the Fréedericksz transition, the coercive torque acts on $\mathbf{C}(\mathbf{r})$ to suppress the NG mode of $\phi(\mathbf{r})$ because of the positive anisotropy of the magnetic susceptibility of the NLC. In the electroconvective state beyond V_c, as there is competition between disorder with the interaction between the convective flow and director and order by this suppression, a certain degree of order occurs depending on the strength of the electric field, which controls the energy injected into the system and the strength of the magnetic field, as shown in Fig. 1(b). Hence, because the magnetic field, which acts on the additional degrees of freedom in liquid crystals, can

*hidaka@ap.kyushu-u.ac.jp

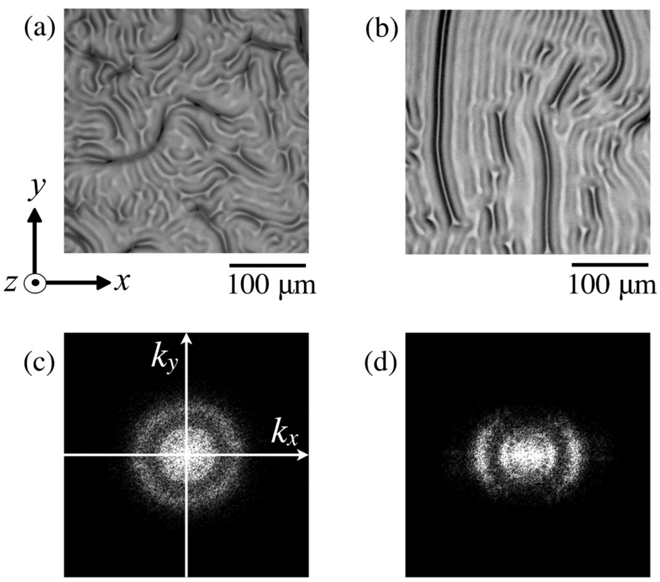

FIG. 1. Electroconvective patterns in a homeotropic nematic system and their 2D power spectra. (a) $H = 0$, $\varepsilon = 0.1$. This pattern corresponds to the SMT. (b) $H = 400\,\mathrm{G}$, $\varepsilon = 0.1$. (c, d) 2D power spectra obtained from (a) and (b), respectively, by fast Fourier transformation.

be used as an external field, which is independent of the generation mechanism of electroconvection, one can study responses of the dissipative structures to external fields. So far, the responses of the SMT to dc magnetic fields [15–18] and step magnetic fields [19] have been studied. However, it is thought that alternating-current (ac) external field responses are more suitable for investigating physical properties of the system, because the SMT is a dynamical phenomenon with several physical time scales. In the present study, therefore, we propose methods to reveal dynamical properties of the SMT obtained from the response to ac magnetic fields.

We introduce an order parameter that quantitatively measures the ordering induced by a magnetic field (Fig. 1). Here we adopt the pattern ordering M_p defined by

$$M_p = \langle \cos 2(\psi - \psi_H) \rangle = \frac{\int_{-\frac{\pi}{2}}^{\frac{\pi}{2}} B(\psi) \cos 2(\psi - \psi_H) \mathrm{d}\psi}{\int_{-\frac{\pi}{2}}^{\frac{\pi}{2}} B(\psi) \mathrm{d}\psi}, \tag{1}$$

where ψ_H denotes the azimuth of the external magnetic field, and $B(\psi)$ the distribution function of the azimuth of $\mathbf{q}(\mathbf{r})$ obtained from the 2D spectrum of the convection pattern. The value of M_p is bounded in $0 \leqslant M_p \leqslant 1$. For a completely isotropic pattern, M_p is equal to 0, and for a completely striped pattern M_p is equal to 1. M_p is based on the magnetization in the 2D *XY* model and the orientational order parameter in NLC [18–20].

II. EXPERIMENTAL AND ANALYSIS

The homeotropic nematic system used in the present research was prepared as follows. The NLC was p-metoxy-benziliden-p'-n-buthyl-annylin (MBBA), which has been a standard material for the study of electroconvection. With its electric conductivity increased by tetra-n-butylammonium bromide, MBBA was enclosed between two glass plates coated with circular transparent electrodes. The nematic director is perpendicular to the electrodes (x-y plane). The distance d between the two electrodes was 42.8 μm, and the diameter of the circular electrode was 12.9 mm. The measurement temperature was stabilized at $30.00 \pm 0.05\,^{\circ}$C.

An ac voltage $V_{\mathrm{ac}} = \sqrt{2}V \cos(2\pi \nu t)$, which was generated by a synthesizer (WF1974; NF, Yokohama, Japan) and amplified by an amplifier (F10A; FLC Electronics, Partille, Sweden), was applied to the NLC perpendicular to the x-y plane (along the z axis). A normalized frequency $\eta \equiv (\nu - \nu_L)/\nu_L$ of the ac voltage was fixed at $\eta = -0.5$. Here, $\nu_L = 700$ Hz is the Lifshitz frequency, corresponding to the absence of a magnetic field, which separates the oblique rolls regime in $\nu < \nu_L$ from the normal rolls regime in $\nu > \nu_L$ [20]. In particular, we performed the present experiments in the oblique rolls regime in a manner similar to that used in Refs. [18] and [19].

The ac magnetic field $H(t) = H_0 \cos(2\pi f_H t)$ generated by an electromagnet (TM-WTV8615C-103; Tamakawa, Sendai, Japan) with a bipolar power supply (BP4610; NF) was applied to the homeotropic nematic system along the x axis. Because the threshold of the magnetic field H_F for the Fréedericksz transition is 950 G, the amplitude H_0 was set to 400 G, which is sufficiently lower than H_F to avoid the influence of the transition. We measured $H(t)$ directly by inserting a probe from a Gauss meter (475DSP; Lakeshore, Columbus, OH).

Temporal sequences of images of the convective patterns were captured using the following procedure. First, we applied voltage $V_F < V < V_c$ to induce the Fréedericksz transition and waited 20 min for $\phi(\mathbf{r})$ to become uniform. Here V_c is the threshold voltage for the occurrence of electroconvection in the absence of a magnetic field. Next we increased V to obtain a normalized voltage $\varepsilon \equiv (V^2 - V_c{}^2)/V_c{}^2 = 0.1$ and waited 10 min for transient behavior of the convective state to die away. Then we applied the ac magnetic field $H(t)$ to the homeotropic nematic system and waited 20 min until the stationary convective state appeared. We captured images of the convective patterns using a CCD camera (Retiga 2000R; QImaging, Surrey, Canada) controlled by software (QCAPTURE PRO v.5; QImaging). Upon capturing the images, we set the sampling time Δt so that the number of measuring points $1/f_H\,\Delta t$ included in a cycle of $H(t)$ was larger than 16. In addition, we set the total measuring time T so that the total number $T f_H$ of cycles of $H(t)$ was larger than 20. The image size was 0.684×0.684 mm^2 (1024×1024 pixels). We analyzed the image data using self-made programs and ImageJ [21].

III. RESULTS AND DISCUSSION

Figures 2(a) and 2(b) show typical $M_p(t)$ for low f_H. We found that $M_p(t)$ oscillates at the same frequency as that of $H^2(t) = (H_0{}^2/2)(1 + \cos(2\pi \cdot 2 f_H t))$. This phenomenon can be traced from the interaction energy between the director $\mathbf{n}$ and the magnetic field $\mathbf{H}$, written as $-(1/2)\Delta\chi(\mathbf{H}\cdot\mathbf{n})^2$, where $\Delta\chi$ is the anisotropy of the magnetic susceptibility of NLC. As mentioned above, the projection of the director $\mathbf{n}$ in the x-y

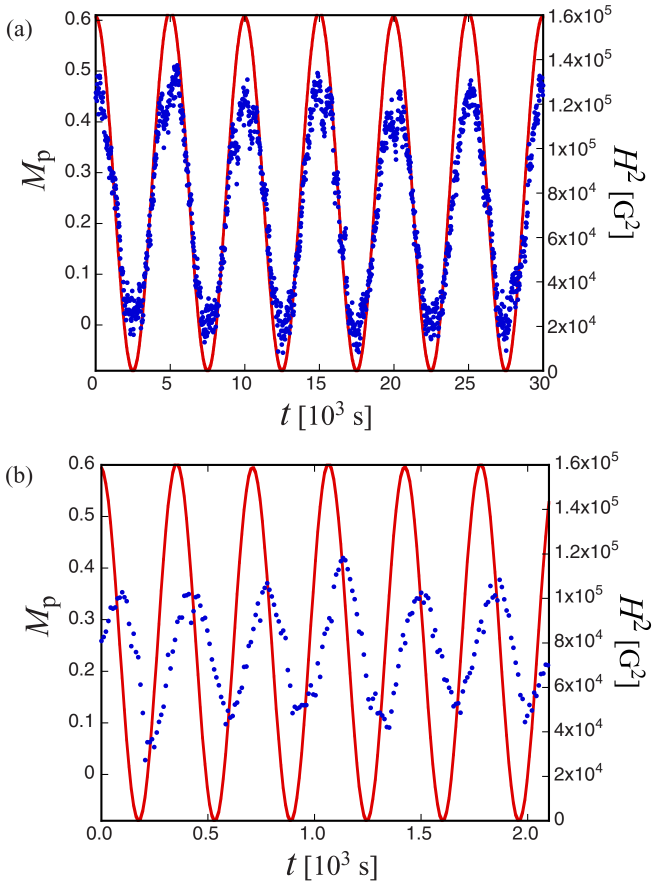

FIG. 2. (Color online) $M_p(t)$ for $f_{\rm eff} = 0.2$ mHz (a) and $f_{\rm eff} = 2.8$ mHz (b). Filled (blue) circles represent $M_p(t)$, and solid (red) lines show $H^2(t)$.

plane is the $\mathbf{C}(\mathbf{r})$ director, and the electroconvection occurs as a consequence of the nonlinear interaction between $\mathbf{C}(\mathbf{r})$ and $\mathbf{q}(\mathbf{r})$. Therefore, $\mathbf{q}(\mathbf{r})$ oscillates synchronously with $H^2(t)$. Consequently, $M_p(t)$, as the pattern ordering of the azimuth of $\mathbf{q}(\mathbf{r})$, oscillates at the same frequency as that of $H^2(t)$.

As there are no higher harmonic components in the power spectra of $M_p(t)$ for low f_H, they can be described as

$$M_p(t) = M_{p0}\cos(2\pi f_{\rm eff}t - \delta) + M_{p1}, \tag{2}$$

where $f_{\rm eff} = 2f_H$ [22]. Since $M_p(t)$ is bounded between 0 and 1 and responses to $H^2(t)$, the constant M_{p1} is necessary. The phase difference δ and the amplitude M_{p0} were obtained from the values of the maximum and minimum of $M_p(t)$ and $H^2(t)$ as follows. The time delay of a maximum (minimum) of $M_p(t)$ to the corresponding maximum (minimum) of $H^2(t)$ was obtained. δ was obtained from the mean value of all the time delays. The difference between a maximum value and the next minimum value of $M_p(t)$ was obtained. M_{p0} is the mean value corresponding to half the difference.

Figure 3 shows the $f_{\rm eff}$ dependence of M_{p0}^2. The result that a discontinuous change appears at $f_{\rm eff} \simeq 6$ mHz suggests that the behavior in the high-$f_{\rm eff}$ regime is different from that in the low-$f_{\rm eff}$ regime. Indeed, $M_p(t)$ deviates from Eq. (2), an issue we return to below. Therefore, a different analysis method should be adopted for each frequency regime.

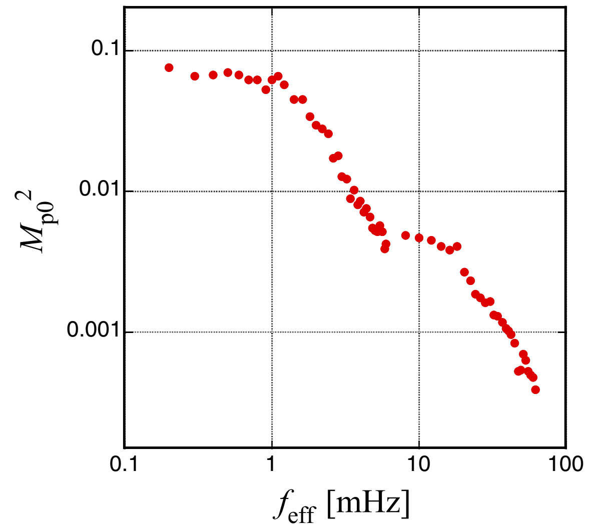

FIG. 3. (Color online) Dependence of M_{p0}^2 on $f_{\rm eff}$ plotted on a logarithmic scale.

In Ref. [18], the pattern susceptibility for dc magnetic fields was introduced to investigate the effects of external forces to convective patterns. For the present study, we also define the pattern susceptibility χ_p by

$$\tilde{M}_p(t) = \chi_p F(t), \tag{3}$$

where $\chi_p \equiv \chi_p' + i\chi_p''$ is a complex number, and $\tilde{M}_p(t) \equiv M_p(t) - M_{p1}$. The external force $F(t)$ is represented by

$$F(t) = h_0 \cos(2\pi f_{\rm eff}\, t). \tag{4}$$

χ_p is expressible in terms of δ and M_{p0},

$$\chi_p' = \tfrac{M_{p0}}{h_0}\cos\delta, \tag{5}$$

$$\chi_p'' = \tfrac{M_{p0}}{h_0}\sin\delta, \tag{6}$$

where $h_0 = H_0{}^2/2$. The $f_{\rm eff}$ dependence of χ_p, which is obtained from the results of δ and M_{p0} using Eqs. (5) and (6), is shown in Fig. 4.

In modeling the behavior for low $f_{\rm eff}$, we use a linear relaxation model with an external force [1],

$$\frac{\rm d}{{\rm d}t}\tilde{M}_p(t) = -\frac{1}{\tau}\tilde{M}_p(t) + \frac{\chi_p'(0)}{\tau}F(t), \tag{7}$$

where τ is the relaxation time. For $f_{\rm eff} \to 0$, $\tilde{M}_p(t) = \chi_p'(0)F(t)$. Substituting Eq. (3) into Eq. (7), we obtained the Debye-type relaxation spectra [1]:

$$\chi_p'(f_{\rm eff}) = \frac{\chi_p'(0)}{1 + (2\pi f_{\rm eff}\tau)^2}, \tag{8}$$

$$\chi_p''(f_{\rm eff}) = \frac{2\pi f_{\rm eff}\tau \cdot \chi_p'(0)}{1 + (2\pi f_{\rm eff}\tau)^2}. \tag{9}$$

We performed fittings of χ_p to Eqs. (8) and (9) in $f_{\rm eff} \lesssim 6$ mHz. As shown in Fig. 4, the experimental results for χ_p' and χ_p'' in this frequency regime fit well with Eqs. (8) and (9), respectively. From these fits, we obtain a relaxation time τ_r of 97 ± 5 s from χ_p' and τ_i of 107 ± 5 s from χ_p''.

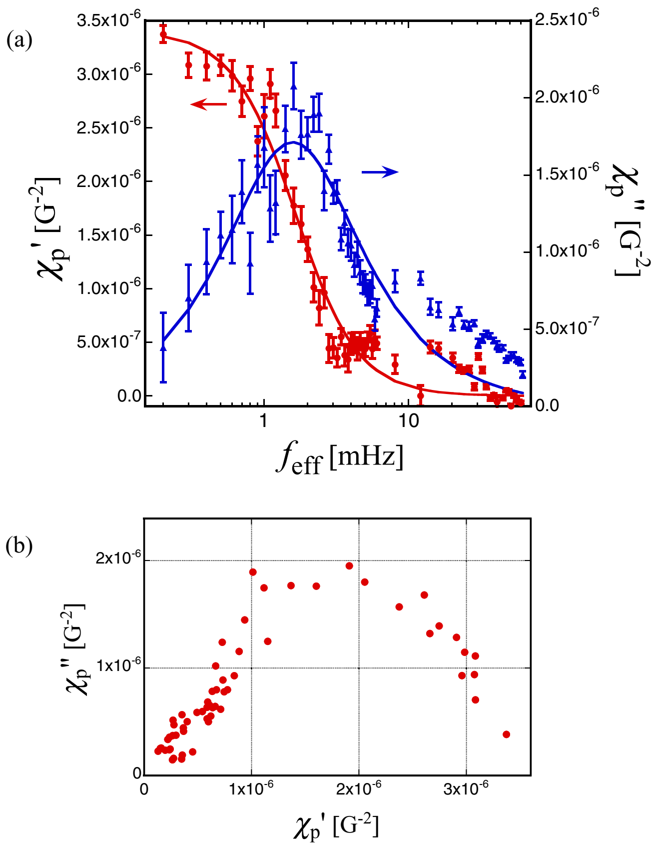

FIG. 4. (Color online) (a) Dependences of χ_p' [(red) circles] and χ_p'' [(blue) triangles] on f_{eff}. f_{eff} is represented on a logarithmic scale. Solid lines show fittings to Eqs. (8) and (9). $\chi_p'(0) = 3.4 \times 10^{-6}$ G^{-2} was obtained by the fitting. (b) Relation between $\chi_p'(f_{\mathrm{eff}})$ and $\chi_p''(f_{\mathrm{eff}})$ plotted using f_{eff} as a common parameter (Cole-Cole plot).

In Fig. 4(b), the relationship between $\chi_p'(f_{\mathrm{eff}})$ and $\chi_p''(f_{\mathrm{eff}})$ is plotted using f_{eff} as a common parameter. Called a Cole-Cole plot [23], this plot for the Debye-type relaxation forms a perfect semicircle [1]. In the present case, the left side of the plot, corresponding to high f_{eff}, deviates from a perfect semicircle. However, because the data points seem to follow some function, a detailed analysis may help to clarify the complex dynamics [24].

As shown in Fig. 4, the results of χ_p do not coincide with Eqs. (8) and (9) for $f_{\mathrm{eff}} \gtrsim 6$ mHz. In this regime, $M_p(t)$ also deviates from Eq. (2) and has slow and large fluctuations other than the oscillation with f_{eff} (see Fig. 5). To observe this fluctuation, we introduce the dynamic order parameter, defined as the average of $M_p(t)$ over one period,

$$M_i = \frac{1}{T_{\mathrm{eff}}} \int_{(i-1)T_{\mathrm{eff}}}^{iT_{\mathrm{eff}}} M_p(t')\, dt', \tag{10}$$

where $i = 1,2,3,\ldots$ and $T_{\mathrm{eff}} = 1/f_{\mathrm{eff}}$ [22]. At $t' = 0$ s, $M_p(t)$ shows the first maximum. From Fig. 5, M_i can sufficiently capture the large fluctuation of $M_p(t)$. Moreover, we evaluated the magnitude of the fluctuations using the variance $S^2 = \langle (M_i - \langle M_i \rangle)^2 \rangle$ of M_i, where $\langle \cdots \rangle$ denotes the average on i. From the dependence of S^2 on f_{eff} (Fig. 6), the fluctuation in M_i increases with f_{eff}. This means that the periodically oscillating force with high f_{eff} induces slow and

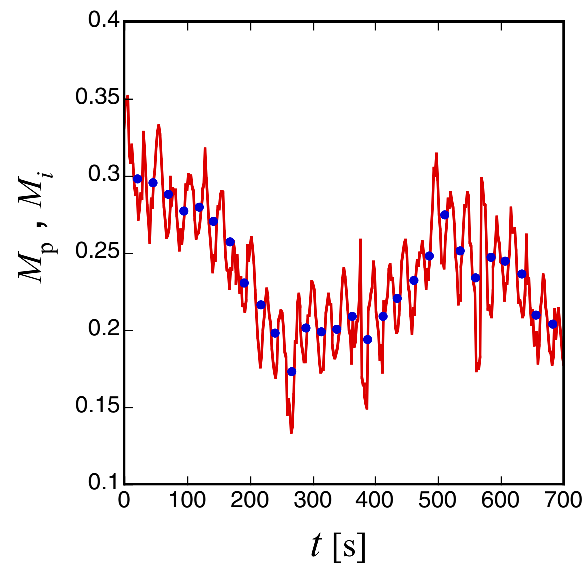

FIG. 5. (Color online) Typical $M_p(t)$ [solid (red) line] shown in the high-f_{eff} regime and M_i [(blue) circles] obtained from Eq. (10). $f_{\mathrm{eff}} = 40$ mHz. M_i data are plotted at $t = iT_{\mathrm{eff}}$.

large fluctuations of $M_p(t)$ other than the oscillation with f_{eff}. If the present system is governed by the linear relaxation model of Eq. (7) over the whole f_{eff} regime, M_{p0} becomes smaller and M_{p1} is kept constant also for high f_{eff}. The result shown in Fig. 6 suggests that the nonlinearity revealed in high f_{eff} induces the slow and large fluctuations of $M_p(t)$.

Let us again consider a substance that is composed of polar molecules with permanent dipoles. The orientation of the molecule is thermally fluctuating. If the orientation of the molecule oscillates by applying an ac electric field to this substance, energy given by the electric field is dissipated by friction among the rotating molecules, and the dissipation is described by the imaginary part of the response function. In this case, the thermal fluctuations under no electric field and the

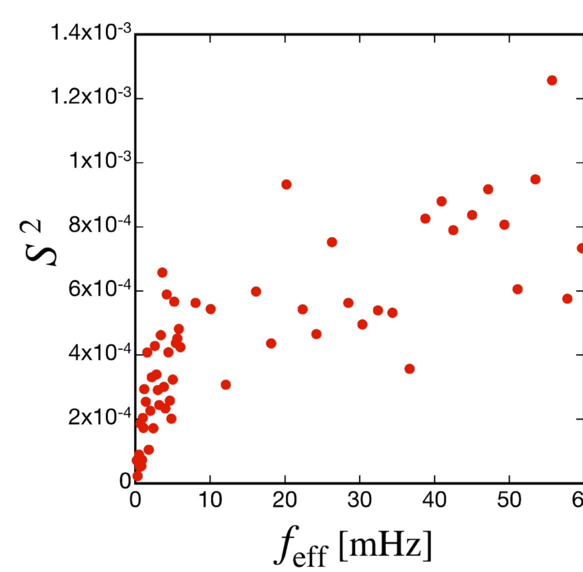

FIG. 6. (Color online) Dependence of the variance S^2 of M_i on f_{eff}.

response function are associated by the fluctuation-dissipation theorem [1]. In the SMT, in contrast, the direction of convective rolls is always fluctuating because of interactions between the convection and the molecular orientation, as stated earlier. In this state, energy injected by applying electric fields is dissipated by the molecular viscosity of the NLC. In the present study, the chaotic convective patterns are ordered by applying magnetic fields. Then the interactions which induce the STC act as "friction" for the ordering. We obtained the imaginary part of the complex pattern susceptibility for the responses to the oscillating external force as shown in Fig. 4. This suggests that the energy given by the external force induces a new type of dissipation which is different from that caused by the molecular viscosity. However, the relation between the complex pattern susceptibility and the chaotic fluctuations of convective patterns has not been revealed yet. Recently, additional friction as a result of chaos has been researched as a new subject in statistical mechanics [10,25–28]. In the future, the fluctuation-dissipation relation in nonequilibrium open systems may become an important aspect in clarifying transport phenomena arising from such chaos-induced friction.

IV. SUMMARY

We have studied the responses to ac magnetic fields of SMT, a form of STC, in electroconvection of nematics. The results are summarized as follows. We measured the dynamical responses using temporal changes of the order parameter $M_p(t)$, which indicates the degree of ordering in a convective pattern induced by the magnetic field $H(t)$. $M_p(t)$ oscillates at frequency $f_{\rm eff}$, which is equal to that of the square of the magnetic field $H^2(t)$ and which can be explained by the properties of the liquid crystal for magnetic fields. The amplitudes M_{p0} of $M_p(t)$ and the phase differences δ between $M_p(t)$ and $H^2(t)$ were obtained by changing $f_{\rm eff}$. We calculated the complex susceptibility χ_p of the pattern from M_{p0} and δ. We introduced the linear relaxation model to explain the $f_{\rm eff}$ dependence of χ_p for the low-$f_{\rm eff}$ regime and obtained the relaxation time by fittings to the Debye-type relaxation spectra. In the high-$f_{\rm eff}$ regime, because slow and large fluctuations of $M_p(t)$ other than the oscillation with $f_{\rm eff}$ appear, χ_p does not fit the relaxation spectra. The magnitude of this fluctuation increases with increasing $f_{\rm eff}$.

In the present study, we have evaluated the responses of convective patterns using the global order parameter M_p, which is a spatially averaged variable. However, to clarify the response dynamics in more detail, especially for the higher $f_{\rm eff}$ regime, a local measurement should be performed. Therefore, it will be necessary to introduce the azimuth $\psi(\mathbf{r})$ of the local wave vector [29].

ACKNOWLEDGMENTS

This work was supported by JSPS KAKENHI Grant Nos. 24540408 and 15K05799.

[1] R. Kubo, M. Toda, and N. Hashitsume, *Statistical Physics II, Nonequilibrium Statistical Mechanics* (Springer-Verlag, Berlin, 1991).
[2] P. C. Hohenberg and B. I. Shraiman, Physica D **37**, 109 (1989).
[3] M. C. Cross and P. C. Hohenberg, Rev. Mod. Phys. **65**, 851 (1993).
[4] Y. Hidaka and N. Oikawa, FORMA **29**, 29 (2014).
[5] A. Hertrich, W. Decker, W. Pesch, and L. Kramer, J. Phys. II France **2**, 1915 (1992).
[6] P. G. de Gennes and J. Prost, *The Physics of Liquid Crystals*, 2nd ed. (Oxford University Press, New York, 1993).
[7] A. G. Rossberg, A. Hertrich, L. Kramer, and W. Pesch, Phys. Rev. Lett. **76**, 4729 (1996).
[8] Y. Hidaka, K. Tamura, and S. Kai, Prog. Theor. Phys. Suppl. **161**, 1 (2006).
[9] F. Nugroho, T. Narumi, Y. Hidaka, J. Yoshitani, M. Suzuki, and S. Kai, Phys. Rev. E **85**, 030701 (2012).
[10] T. Narumi, J. Yoshitani, M. Suzuki, Y. Hidaka, F. Nugroho, T. Nagaya, and S. Kai, Phys. Rev. E **87**, 012505 (2013).
[11] K. Tamura, Y. Yusuf, Y. Hidaka, and S. Kai, J. Phys. Soc. Jpn. **70**, 2805 (2001).
[12] K. Tamura, Y. Hidaka, Y. Yusuf, and S. Kai, Physica A **306**, 157 (2002).
[13] Y. Hidaka, Y. Hosokawa, N. Oikawa, K. Tamura, R. Anugraha, and S. Kai, Physica D **239**, 735 (2010).
[14] M. Suzuki, H. Sueto, Y. Hosokawa, N. Muramoto, T. Narumi, Y. Hidaka, and S. Kai, Phys. Rev. E **88**, 042147 (2013).
[15] H. Richter, N. Klöpper, A. Hertrich, and Á. Buka, Europhys. Lett. **30**, 37 (1995).
[16] J.-H. Huh, Y. Hidaka, and S. Kai, J. Phys. Soc. Jpn. **68**, 1567 (1999).
[17] N. Éber, S. Németh, A. G. Rossberg, L. Kramer, and A. Buka, Phys. Rev. E **66**, 036213 (2002).
[18] F. Nugroho, Y. Hidaka, T. Ueki, and S. Kai, J. Phys. Soc. Jpn. **79**, 123001 (2010).
[19] F. Nugroho, Y. Hidaka, T. Ueki, and S. Kai, J. Phys. Soc. Jpn. **81**, 024004 (2012).
[20] R. Anugraha, K. Tamura, Y. Hidaka, N. Oikawa, and S. Kai, Phys. Rev. Lett. **100**, 164503 (2008).
[21] C. A. Schneider, W. S. Rasband, and K. W. Eliceiri, Nat. Meth. **9**, 671 (2012).
[22] B. K. Chakrabarti and M. Acharyya, Rev. Mod. Phys. **71**, 847 (1999).
[23] K. S. Cole and R. H. Cole, J. Chem. Phys. **9**, 341 (1941).
[24] D. W. Davidson and R. H. Cole, J. Chem. Phys. **18**, 1417 (1950).
[25] H. Mori and H. Fujisaka, Phys. Rev. E **63**, 026302 (2001).
[26] H. Mori and M. Okamura, Phys. Rev. E **76**, 061104 (2007).
[27] M. Okamura and H. Mori, Phys. Rev. E **79**, 056312 (2009).
[28] H. Mori and M. Okamura, Phys. Rev. E **80**, 051124 (2009).
[29] K. Tamura, R. Anugraha, R. Matsuo, Y. Hidaka, and S. Kai, J. Phys. Soc. Jpn. **75**, 063801 (2006).